Polym. Bull. (2018) 75:5535–5549
https://doi.org/10.1007/s00289-018-2333-y

ORIGINAL PAPER

Experimental investigation on the yield behavior of PMMA

Ji Qiu[1,2] · Tao Jin[1,2] · Buyun Su[1,2] · Xuefeng Shu[1,2] · Zhiqiang Li[1,2,3]

Received: 24 October 2017 / Revised: 10 March 2018 / Accepted: 4 April 2018 /
Published online: 25 April 2018

Abstract Quasi-static compression, tension and combined shear–compression tests were conducted to characterize the mechanical behavior of PMMA. The cylinder samples and dog-bone samples were used for uniaxial testing. The shear–compression samples of four different angles (15°, 30°, 45°, and 50°) were used to obtain the multiaxial stress state instead of complex loading equipment. The yield behaviors of PMMA cannot be described by the Tresca or Mises criterion due to the effects of both the first invariant of the stress and the third invariant of deviatoric stress. A criterion is proposed that includes the first invariant of the stress and the third invariant of deviatoric stress in this paper. In other word, the effects of hydrostatic pressure and Lode angle are considered. The proposed yield criterion has the capability to precisely capture the experimental yield loci of PMMA.

Keywords PMMA · Combined shear–compression sample · Yield criterion · The third invariant of deviatoric stress · Hydrostatic pressure

Introduction

PMMA (polymethyl-methacrylate) is a kind of low-cost and light-weight material with excellent physical and optical properties. It is widely used in aviation, architecture, biomedicine and other fields [1–4]. Many previous literatures have

✉ Xuefeng Shu
shuxuefeng@tyut.edu.cn

1 Institute of Applied Mechanics and Biomedical Engineering, Taiyuan University of Technology, Taiyuan 030024, China

2 Shanxi Key Laboratory of Material Strength and Structural Impact, Taiyuan 030024, China

3 State Key Laboratory of Explosion Science and Technology (Beijing Institute of Technology), Beijing, China

made contributions to the understanding of the uniaxial mechanical properties of PMMA. Holmquist et al. [5] had presented the response of polymethyl methacrylate (PMMA) subjected to large strains, high strain rates, high pressures, a range in temperatures, and variations in the intermediate principal stress. Richeton et al. [6] investigated that uniaxial compression stress–strain tests were carried out on three commercial amorphous polymers. Chen et al. [7] researched the mechanical behavior of PMMA under uniaxial tension and compression loading conditions. The results show that the compressive strength is higher than tensile strength. Jerabek et al. [8] investigated and compared the pre- and post-yield regime by two uniaxial compression test methods. Wu.et al. [9] investigated the PMMA tensile capability at a medium strain rate and found that the strain rate greatly influenced these properties. Additionally, the yield behavior of PMMA exhibit obvious strain rate and temperature sensitivity, which have been substantiated by many experimental investigations. Methiesen et al. [10] described the glass transition through temperature-dependent material properties. Richeton et al. [11] found that the initial Young's modulus is forcefully affected by strain rates. Nasrouri et al. [12] investigated the effect of strain rate, temperature, and adiabatic heating on the mechanical behavior of PMMA and the negative correlation between temperature and the PMMA yield stress was found. It should be noted that PMMA may be subjected to complex multiaxial stress states under actual circumstances. Therefore, it is essential to analyze the multiaxial yield behavior of PMMA and establish a yield criterion based on multiaxial experimental results. Forquin et al. [13] investigated the confined behavior of PMMA by quasi-oedometric compression. They adopted the cylindrical PMMA specimens enclosed in a brass or high-strength aluminium alloy confinement vessel. Jin et al. [14] investigated compression–shear failure behavior of PMMA using a cylindrical specimen with beveled ends of different angles and experimental results show that the failure force of PMMA decreased as the tilt angle of the specimen increased. Zhou et al. [15] used complex loading equipment to achieve the combined shear–compression stress state and different kind of combined shear–compression experiments were achieved through changing pressure head angle. On the other hand, many researches indicated that the Tresca and Mises criterion cannot give an appropriate description of the yield behavior of PMMA. Because the yield behaviors of PMMA affected by first invariant of stress tensor (I_1) and third invariant of deviatoric stress (J_3) [16, 17]. Therefore, Farrokh et al. [18] proposed a strain rate sensitivity yield criterion $f(I_1, J_2)$ by experimental investigation. The relationship between I_1 and $\sqrt{J_2}$ is liner. It does not have a high capability of charactering the main deformation mechanism of relating shear banding. Ghorbel [19] proposed a viscoplastic constitutive model for polymeric materials based on the parabolic Drucker and Prager criterion. The criterion that was proposed by Ghorbel includes the effects of the first invariant of the stress, the second invariant of deviatoric stress (J_2) and the third invariant of deviatoric stress, respectively.

From the above discussions, it can be concluded that the multiaxial experimental data of the PMMA are limited. Especially, the configuration of yield criterion has not yet been clearly understood. Therefore, present research employs a new test method (i.e., shear–compression samples [20]) to explore the multiaxial yield behavior of PMMA. Furthermore, a yield criterion is extended to include a quadratic I_1 term for accurately predicting the yield locus of PMMA.

Experimental procedure

The test samples were machined by ordinary commercial PMMA bar (Φ 10 mm $\times$ 1000 mm). In this paper, the shear–compression specimen (SCS) was used to generate the additional shear, then the stress state can be controlled by changing the angle of the sample (SCS) which is named loading angle. That is, a slot with a certain angle is introduced on the surface of the cylinder sample. There are four kinds of loading angle α in this paper: 15°, 30°, 45°, 50°. In addition, this investigation applied the cylindrical specimen and dog-bone specimen to obtain the mechanical behavior of compression and tensile. The specific sizes of tested samples are shown in Figs. 1 and 2.

Combined shear–compression and uniaxial tensile/compressive tests were conducted by the universal materials testing machine (CMT5105A, SANS, Shenzhen, PRC) with the load cell of 100 kN. The loading rate is 6 mm/min with the corresponding nominal strain rate of $\dot{\varepsilon} = 0.01\ \mathrm{s}^{-1}$. The specimen was located between two metal heads. The lower end surface of the specimen is limited in the direction of compression (tension), and the upper end surface of the specimen is subjected to the displacement boundary condition. The loading and displacement signals of the specimen during testing were recorded by a computer for subsequent data processing.

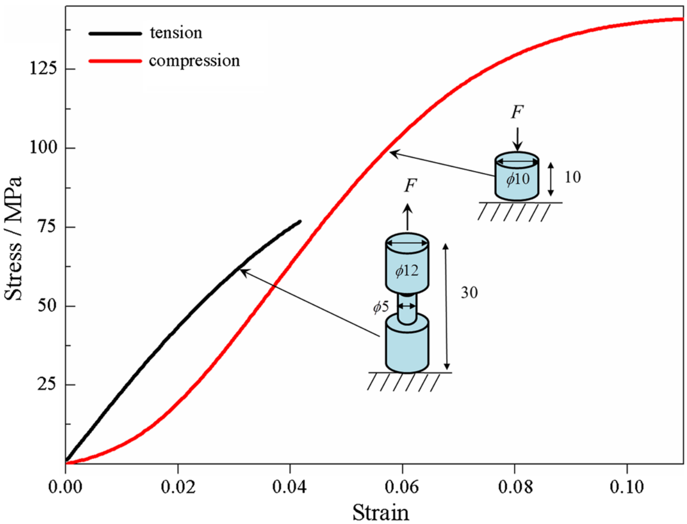

Fig. 1 Schematic of compression and tension specimens

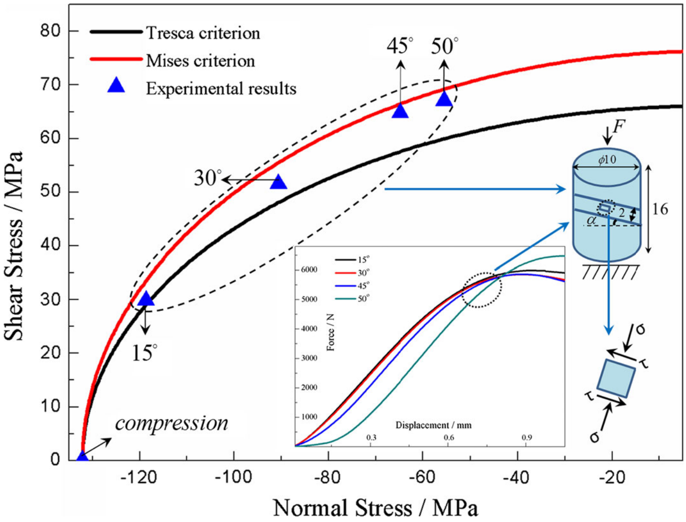

Fig. 2 Schematic of SCS and the yield loci in shear–compression stress space

Results

The compression and tensile nominal stress–strain curves exhibit nonlinear elastic behavior before the yielding. The softening behavior is observed after the yield point. Stress and strain of tension and compression can be calculated from the following equations and as plotted in Fig. 1.

$$\sigma_n = \frac{F_{UTM}}{A_0}, \quad \varepsilon_n = \frac{S}{L} \tag{1}$$

Where F_{UTM} and S are the load and displacements obtained by the universal testing machine, respectively, A_0 and L are original cross-sectional area and the height of specimen. VURAL et al. [21] provided the state of stress at a point within the gage section for the SCS geometry, as shown in Fig. 2. The normal stress σ_n and shear stress τ can be written as:

$$\sigma_n = \frac{F_{UTM}}{Dt}\cos^2\alpha, \quad \tau = \frac{F_{UTM}}{Dt}\cos\alpha\sin\alpha. \tag{2}$$

Rather detailed explanations of the stress state and derivations of the expressions can be found in the previous literature. Similarly, the corresponding normal strains ε_n and shear strains γ_s can be given by the following equations:

$$\varepsilon_n = \frac{S}{h}\cos^2\alpha, \quad \gamma_s = \frac{S}{h}\cos\alpha\sin\alpha \tag{3}$$

Where D and t are the diameter and the thickness of the gage section of SCS, S and h are the displacement of SCS recorded by the universal materials testing machine and the height of the gage section, respectively. The additional $h = \frac{w}{\cos\alpha}$ and $w = 2$ is

Table 1 Values of yield stresses and invariants under different loading conditions

	Compression (MPa)	Tensile (MPa)	SCS			
			15°	30°	45°	50°
Compression component (MPa)	–	–	− 118.73	− 90.63	− 64.83	− 55.54
Shear component (MPa)	–	–	29.85	51.54	64.83	67.05
σ_1 (MPa)	0	70.25	7.08	23.31	40.06	44.80
σ_2 (MPa)	–	–	–	–	–	–
σ_3 (MPa)	− 132.13	0	− 125.81	− 113.94	− 104.90	− 100.34
I_1 (MPa)	− 132.13	70.25	− 118.73	− 90.63	− 64.83	− 55.54
$\sqrt{J_2}$ (MPa)	76.28	40.56	74.77	73.45	74.85	74.32
$\sqrt[3]{J_3}$ (MPa)	− 55.49	29.50	− 54.20	− 51.35	− 48.06	− 45.78

the width of the gage section of all the SCS. Based on above analyzing components of compression and shear stresses are listed in Table 1. Then the maximum principal stress $\sigma_{\max}$ and the minimum principal stress $\sigma_{\min}$ under the shear–compression conditions can be expressed as flowing:

$$\left.\begin{matrix}\sigma_{\max}\\ \sigma_{\min}\end{matrix}\right\} = \frac{\sigma}{2} \pm \left[\left(\frac{\sigma}{2}\right)^2 + \tau^2\right]^{\frac{1}{2}}. \tag{4}$$

The principal stresses under different loading condition are given in Table 1. The tensile stress is generally assumed as a positive value and the compressive stress is opposite. The principal stress value $\sigma_1 > \sigma_2 > \sigma_3$ is also assumed and in other word $\sigma_1 = \sigma_{\max}$ and $\sigma_3 = \sigma_{\min}$. The first invariant of stress, the second invariant of the deviatoric stress and the third invariant of the deviatoric stress are denoted by I_1, J_2 and J_3, respectively, which written as:

$$I_1 = \mathrm{tr}(\sigma_{ij}), \;\; J_2 = \frac{1}{2} \cdot \mathrm{tr}(s_{ij}^2), \;\; J_3 = \frac{1}{3} \cdot \mathrm{tr}(s_{ij}^3) \tag{5}$$

Where the $s_{ij} = \sigma_{ij} - \frac{I_1}{3} \cdot \mathbf{I}$ is deviatoric stress tensor and $\mathbf{I}$ is the second order unit tensor. As discussed above, the values of experimental yield stresses, which are obtained in the $I_1 - \sqrt{J_2} - \sqrt[3]{J_3}$ stress space, are tabulated in Table 1.

Discussion

The yield behavior

The comparisons between the experimental yield loci of PMMA and the Tresca, von-Mises criteria in the shear–compression stress space are shown in Fig. 2. Obviously, the two yield criteria may not have the capability to predict the yield behavior of PMMA precisely. Therefore, it is necessary to introduce the correlative parameters into the yield criterion to describe the mechanical behavior of the PMMA materials under multiaxial loading. As mentioned in introduction, different yield criterions have been proposed, i.e., $f(J_2), f(J_2, J_3), f(I_1, J_2)$. As well known, I_1, J_2 and J_3 mean different physical meanings, hydrostatic pressure, shear deformation and directional deformation, respectively [19]. Then different yield criteria are plotted in the principal stress space, as represented in Fig. 3. It indicated that I_1, J_2 and J_3 have significant influence on the shape of yield surface. J_2 is the foundation of yield criteria. It shows a cylinder surface in full stress space for the yield function $f(J_2)$. The influence of hydrostatic pressure is considered for the yield function of $f(I_1, J_2)$ with the yield surface shows conical (linear relation) or ellipsoid surface in full stress space. The yield surface $f(J_2, J_3)$ which takes the effects of Lode angle into consideration is a prismatic surface in full stress space.

The influence of hydrostatic pressure about PMMA yield behavior is explored by plotting the yield loci of PMMA in $I_1 - \sqrt{J_2}$ space. Figure 4 shows the comparison of the D–P criterion and Von-Mises criterion. Obviously, the values of $\sqrt{J_2}$ have significant changes, with the increase of I_1. This phenomenon reveals that the yield behavior of PMMA is hydrostatic sensitive. Therefore, the D–P criterion that considers hydrostatic pressure term has a high capability of describing the yield behavior of PMMA than the Von-Mises criterion.

Furthermore, to analyze the ability of the J_3 to effect the yield behavior, the yield loci was drawn in the $I_1 - \sqrt{J_2} - \sqrt[3]{J_3}$ space. $\sqrt{J_2}$ varies with $\sqrt[3]{J_3}$ as well shown in Fig. 5. The yield loci under the different loading conditions are highlighted in the full stress space as well. Obviously, the effect of J_3 for the yield behavior of PMMA cannot be neglected. It must be emphasized that based on the experimental results in Figs. 4 and 5, the complex stress state can be easily obtained through SCS with different loading angles.

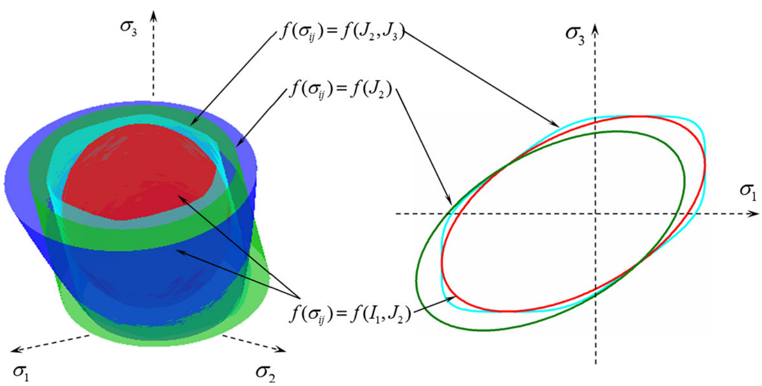

Fig. 3 Yield surfaces of different forms in principal stress space

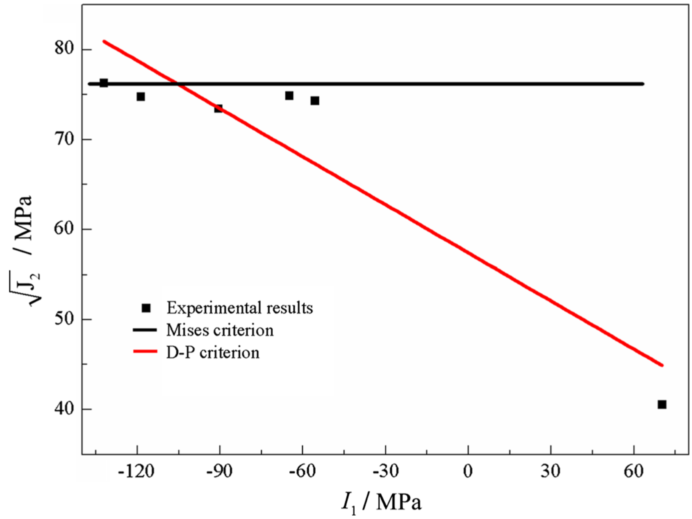

Fig. 4 Yield loci of PMMA in $I_1 - \sqrt{J_2}$ space

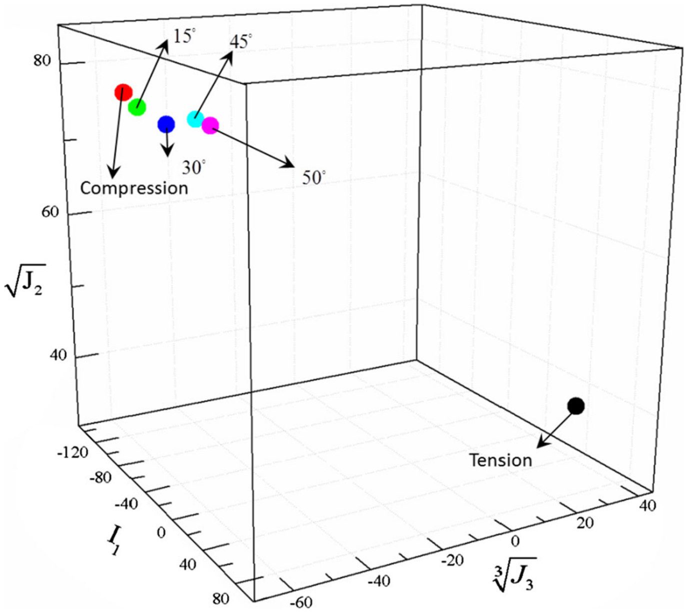

Fig. 5 Yield loci of PMMA in $I_1 - \sqrt{J_2} - \sqrt[3]{J_3}$ space (unit: MPa)

Ghorbel yield criterion

As discussed above, the influences of I_1, J_2, J_3 must be considered simultaneously, when establishing the yield criterion of PMMA. Consequently, Ghorbel [19] proposed a yield criterion, as follows:

$$f = \frac{3J_2}{\sigma_t}\left(1 - \frac{27}{32}\frac{J_3^2}{J_2^3}\right) + \frac{7(m-1)}{8}I_1 - \frac{7}{8}m\sigma_t, \quad m = \frac{\sigma_c}{\sigma_t} \tag{6}$$

Where σ_c and σ_t are compression strength and tension strength, respectively. And m is the ratio of the compression and tension which can be used to describe the asymmetry of the yield surface. Figure 6 compares the yield loci and the yield surface proposed by Ghorbel in the $I_1 - \sqrt{J_2} - \sqrt[3]{J_3}$ pace. Meanwhile, the yield surface shape of the positive view and the side view are given in Fig. 6a, b, respectively. The prediction data slightly deviates from the experimental results. If we choose three principal stress of PMMA instead of the three invariant of the stress and deviatoric stress in Eq. 6, we can rewrite the yield criterion as:

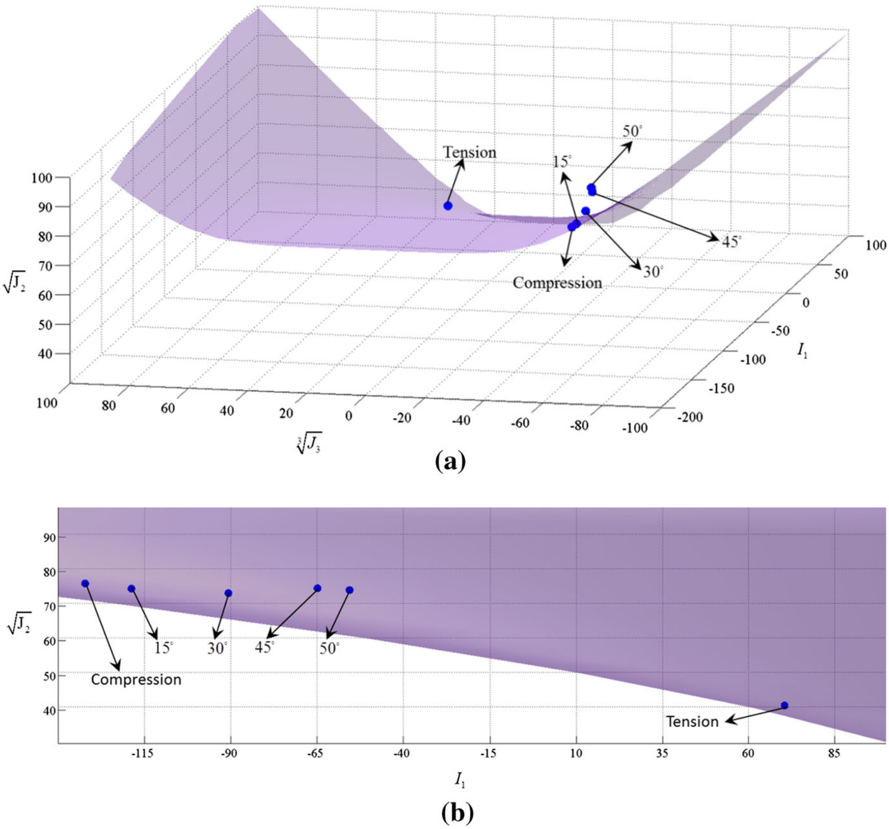

Fig. 6 Yield surface proposed by Ghorbel in $I_1 - \sqrt{J_2} - \sqrt[3]{J_3}$ space, front view (**a**) and side view (**b**) (unit: MPa)

$$
\begin{aligned}
f = & \frac{\left[(\sigma_1-\sigma_2)^2+(\sigma_2-\sigma_3)^2+(\sigma_3-\sigma_1)^2\right]}{2\sigma_{\mathrm{t}}} \\
& \cdot \left(1-\frac{1}{32}\cdot\frac{((2\sigma_1-\sigma_2-\sigma_3)\cdot(2\sigma_2-\sigma_1-\sigma_3)\cdot(2\sigma_3-\sigma_1-\sigma_2))^2}{\left[\frac{(\sigma_1-\sigma_2)^2+(\sigma_2-\sigma_3)^2+(\sigma_3-\sigma_1)^2}{2}\right]^3}\right) \\
& + \frac{7(m-1)}{8}\cdot(\sigma_1+\sigma_2+\sigma_3)-\frac{7}{8}\cdot m\cdot\sigma_{\mathrm{t}}.
\end{aligned}
\tag{7}
$$

Then, the three-dimensional yield surface can be plotted in principal stress space as shown in Fig. 7. It is clear that the shape of yield surface has distinct difference between Ghorbel and Mises yield criteria. The end of yield surface is closed, which indicates that hydrostatic tensile could lead to the yielding of PMMA. In addition, the yield surface on π plane is no longer a circle due to the effect of J_3 and the area of the yield surface on the deviatoric plane changes with hydrostatic pressure axis ($\sigma_1=\sigma_2=\sigma_3$) due to the effect of I_1. Furthermore, the experimental yield loci and theoretical yield surface are plotted in the $\sigma_1-\sigma_3$ stress space as shown in Fig. 8. It can be found that the Ghorbel yield criterion has higher agreement than the Mises yield criterion, especially for the tension and compression asymmetry. However, Ghorbel yield criterion underestimates the yield strength of materials under shear-compressive stress to some extent.

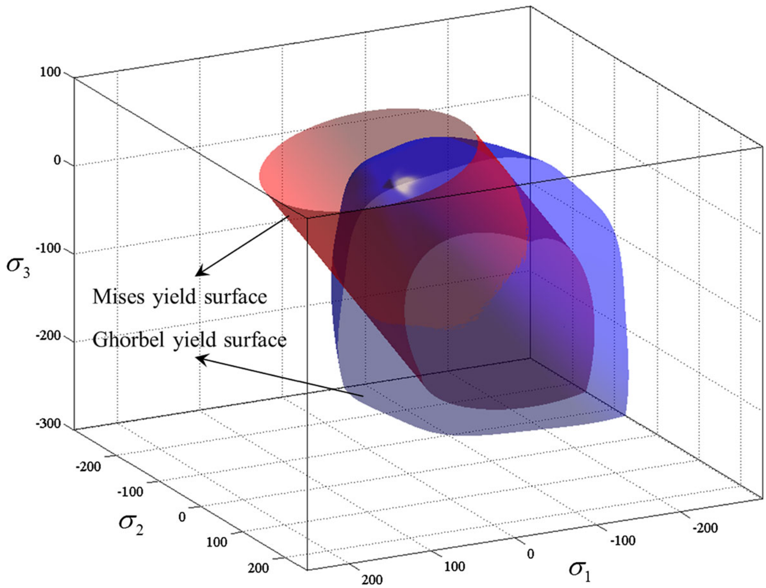

Fig. 7 Mises and Ghorbel yield surfaces in principal stress space (unit: MPa)

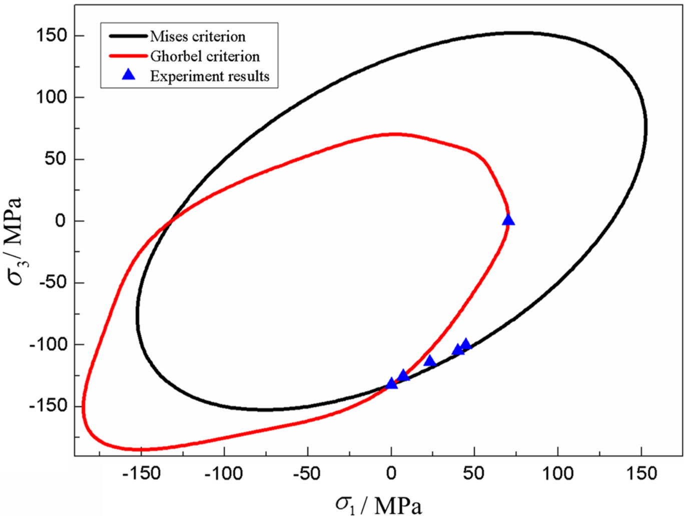

Fig. 8 Comparison between the experimental loci and theoretical yield surfaces (Ghorbel and Mises)

Proposed yield criterion

Ghorbel yield criterion underestimates the yield strength of materials under shear-compressive stress to some extent. This is mainly because Ghorbel yield criterion assumes linear variation between I_1 and J_2. Actually, the relationship is nonlinear as shown in Fig. 9.

Therefore, in this paper, the Ghorbel yield criterion are extended for the PMMA by introducing a quadratic dependence on the I_1. Then, a new yield criterion can be proposed as:

$$f = \frac{a}{\sigma_t} \cdot J_2 \cdot \left(1 - \frac{27}{32} \cdot \frac{J_3^2}{J_2^3}\right) + b \cdot I_1 + \frac{c}{\sigma_t} \cdot I_1^2 - \frac{7}{8} \cdot m \cdot \sigma_{\mathrm{t}}. \tag{8}$$

Here a, b, c are material parameters and can be calibrated by utilizing the experimental results. To solve the three parameters substitute three experimental results (compression, tension, SCS of 45°) substituted into Eq. (8). Then the solution is $a = 1.97$, $b = 0.77$ and $c = 0.30$. Figure 10 compares the difference between the modified yield criterion (see Eq. 8) and the original yield criterion (see Eq. 6).

Obviously, the proposed yield criterion gives better description for the experimental results. Similarly, the proposed yield criterion can be plotted in principal stress pace using the method presented above. One must note here that the new yield surface becomes totally closed, which means that not only biaxial tension can lead to yielding but also biaxial compression can cause yield of PMMA. The quadratic relationship between $\sqrt{J_2}$ and I_1 can be indicated by the yield surface whose both ends are also closed. Meanwhile, the influence of lode angle can be indicated by the noncircular yield surface in the π plane (see Fig. 11).

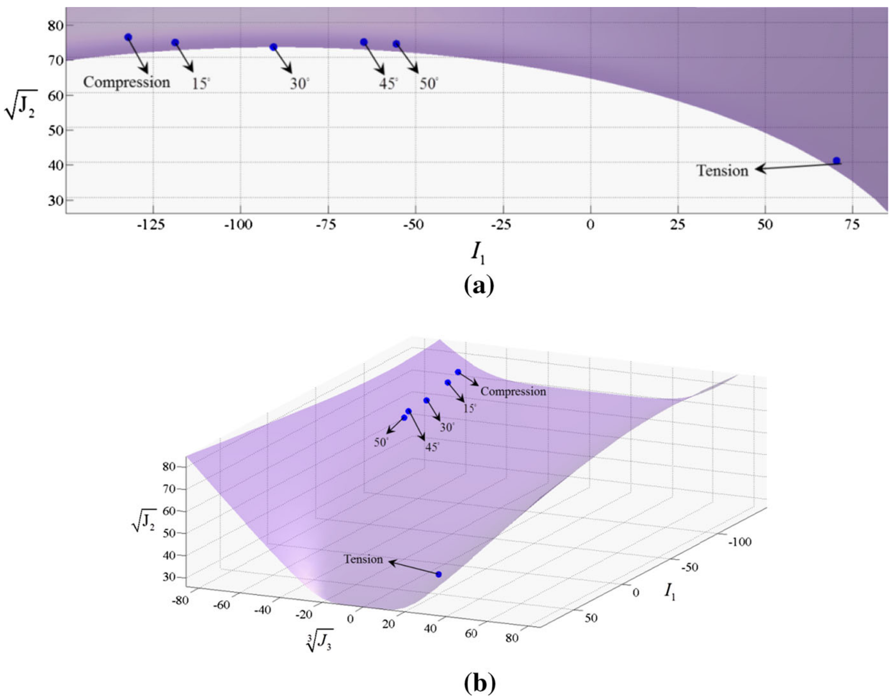

Fig. 9 Yield surface proposed in this paper in $I_1 - \sqrt{J_2} - \sqrt[3]{J_3}$ space, front view (**a**) and side view (**b**) (unit: MPa)

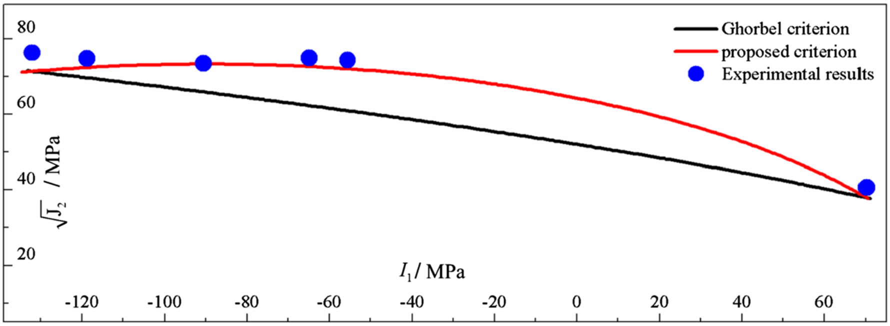

Fig. 10 Comparison between the yield criterion by Ghorbel [16] and present paper in $I_1 - \sqrt{J_2}$ space

The experimental yield data, corresponding yield surfaces obtained from Eqs. 6 and 8 are summarized in $\sigma_1 - \sigma_3$ stress space, as shown in Fig. 12. It is clear that the proposed yield surface accords better with the experimental loci of PMMA than other yield surface.

Furthermore, a series of yield surfaces are summarized in Fig. 13 to investigate the influence of material parameters on the shape of yield surfaces. As the parameter a increases, the yield surface area decreases, namely that parameter a reflects how

Fig. 11 The Ghorbel and the proposed yield surfaces in principal stress space (unit: MPa)

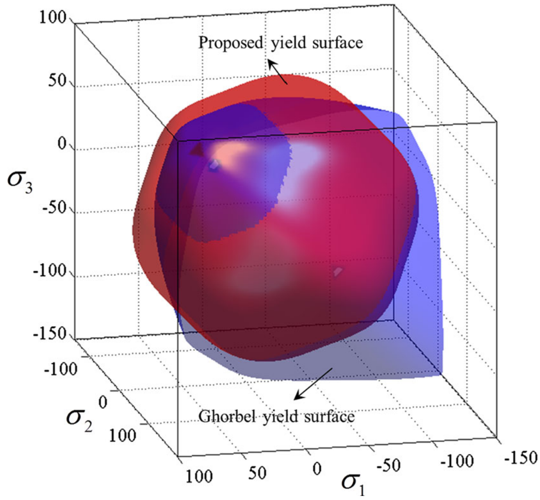

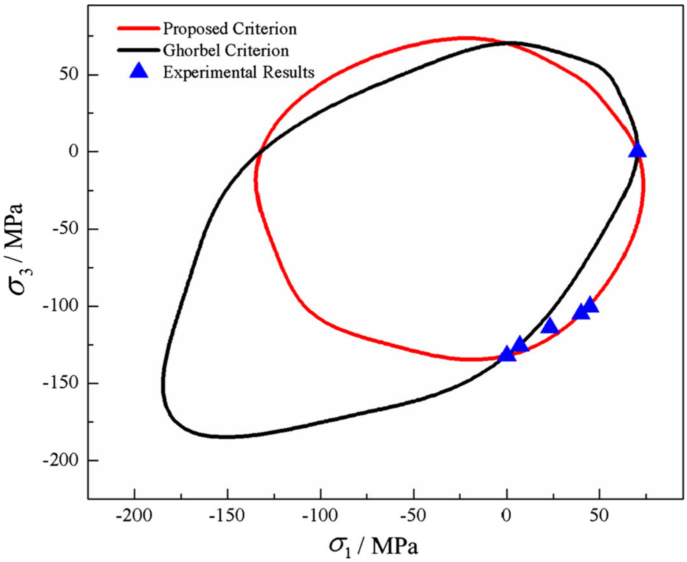

Fig. 12 Experimental yield surface of PMMA in principle stress space

difficulty the materials yield is. However, it has less influence on the biaxial tensile strength. The yield surface offset to third quadrants with increasing parameter b. In other words, the parameter b characterizes the effects on the tension and compression asymmetry. With the increase of parameter c, the yield surface is shrinkage especially in the third quadrant. This result shows that parameter c has a strong influence on biaxial compression.

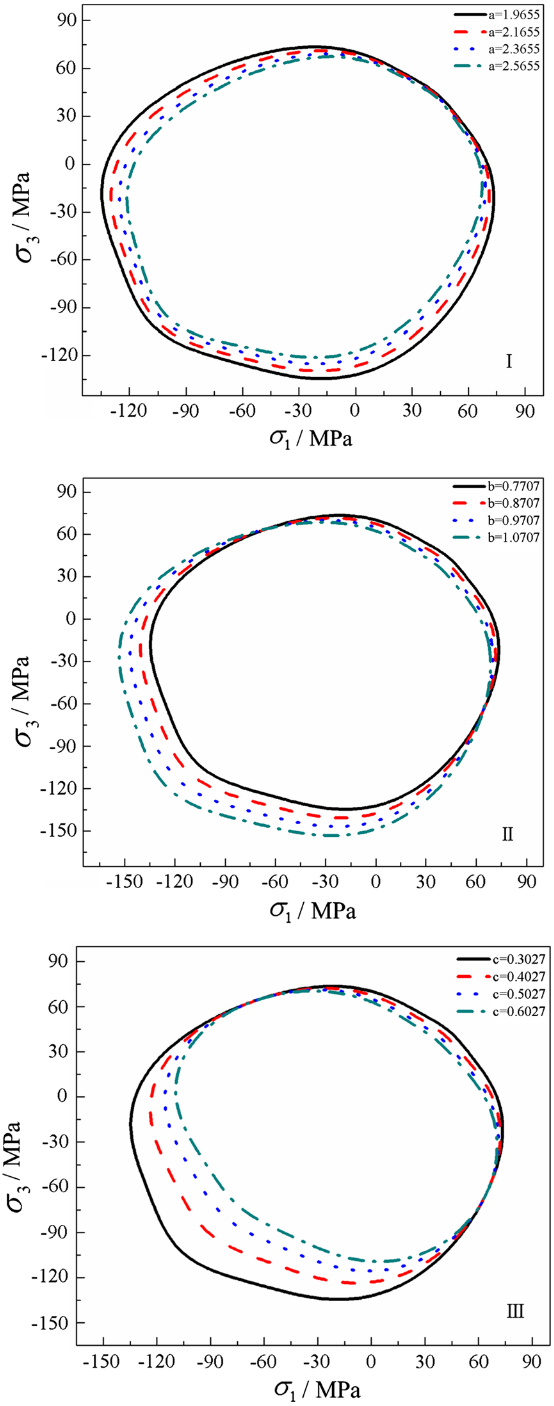

Fig. 13 Effects of materials parameters, i.e., *a* (**I**), *b* (**II**) and *c* (**III**) on the yield surface

Summary

In this paper, the mechanical responses of PMMA under tension, compression and combine shear–compression stress states are investigated by employing the dog-bone sample, cylinder sample and SCS with four different loading angles, respectively. Comparisons between experimental results and Tresca, Mises, D–P, Ghorbel yield criterion predictions are conducted and discussed. The experimental results indicate that the first invariant of the stress and the third invariant of deviatoric stress behave strong influences on the yield behaviors of PMMA. Meanwhile, a modified yield criterion $f(I_1, J_2, J_3)$ that incorporates the quadratic relationship between I_1 and $\sqrt{J_2}$ is proposed in this paper. The accuracy and effectiveness of the proposed yield criterion are verified utilizing the yield data under the complex stress states. Based on the proposed yield criterion, the influences of the material parameters on the shape of yield surfaces have been analyzed. Furthermore, it is indicated that the modified yield criterion provides satisfactory prediction results and expands original scope of applications.

Acknowledgements The authors would like to thank the National Natural Science Foundation of China (Grant nos. 11772217 and 11672199), the School Foundation of Taiyuan University of Technology (no. 2016QN68), the opening project of State Key Laboratory of Explosion Science and Technology (Beijing Institute of Technology, KFJJ16-07M).

References

1. Acharya S, Mukhopadhyay AK (2014) High strain rate compressive behavior of PMMA. Polym Bull 71(1):133–149
2. Jin T, Niu XY, Xiao GS, Wang ZH, Zhou ZW, Yuan GZ, Shu XF (2015) Effects of experimental variables on PMMA nanoindentation measurements. Polym Test 41:1–6
3. Nam JE, Lee JK, Mauldin TC (2010) Isothermal physical aging of thin PMMA films near the glass transition temperature. Polym Bull 65(8):825–835
4. Samad HA, Jaafar M (2009) Effect of polymethyl methacrylate (PMMA) powder to liquid monomer (P/L) ratio and powder molecular weight on the properties of PMMA cement. Polym Plast Technol Eng 48(5):554–560
5. Holmquist TJ, Bradley J, Dwivedi A et al (2016) The response of polymethyl methacrylate (PMMA) subjected to large strains, high strain rates, high pressures, a range in temperatures, and variations in the intermediate principal stress. Eur Phys J Special Top 225(2):343–354
6. Richeton J, Ahzi S, Vecchio KS et al (2006) Influence of temperature and strain rate on the mechanical behavior of three amorphous polymers: characterization and modeling of the compressive yield stress. Int J Solids Struct 43(7):2318–2335
7. Chen W, Lu F, Cheng M (2002) Tension and compression tests of two polymers under quasi-static and dynamic loading. Polym Test 21(2):113–121
8. Jerabek M, Major Z, Lang RW (2010) Uniaxial compression testing of polymeric materials. Polym Test 29(3):302–309
9. Wu HY, Ma G, Xia YM (2004) Experimental study of tensile properties of PMMA at intermediate strain rate. Mater Lett 58:3681–3685
10. Methiesen D, Vogtmann D, Dupaix RB (2014) Characterization and constitutive modeling of stress-relaxation behavior of poly (-methyl methacrylate) (PMMA) across the glass transition temperature. Mech Mater 71:74–84
11. Richeton J, Schlatter G, Vecchio KS, Rémond Y, Ahzi S (2005) A unified model for stiffness modulus of amorphous polymers across transition temperatures and strain rates. Polymer 46:8194–8201

12. Nasraoui M, Forquin P, Siad L, Rusinek A (2012) Influence of strain rate, temperature and adiabatic heating on the mechanical behavior of poly-methyl-methacrylate: experimental and modelling analyses. Mater Des 37:500–509
13. Forquin P, Nasraoui M, Rusinek A et al (2012) Experimental study of the confined behaviour of PMMA under quasi-static and dynamic loadings. Int J Impact Eng 40:46–57
14. Jin T, Zhou ZW, Wang ZH, Wu GY, Liu ZG, Shu XF (2015) Quasi-static failure behaviour of PMMA under combined shear-compression loading. Polym Test 42:181–184
15. Zhou ZW, Su BY, Wang ZH, Li ZQ, Shu XF, Zhao LM (2015) Shear-compression failure behavior of PMMA at different loading rates. Mater Lett 109:151–153
16. Tresca H (1864) Mémoire sur l'écoulement des corps solides soumis à de fortes pressions. C R Acad Sci Paris 59:754–758
17. Von Mises R (1913) Mechanik der festen Körper im plastisch deformablen Zustand, Nachrichten von der Gesellschaft der wissenschaften zu Göttingen. Math Phys Klasse 1:582–592
18. Farrokh B, Khan AS (2010) A strain rate dependent yield criterion for isotropic polymers: low to high rates of loading. Eur J Mech A Solids 29(2):274–282
19. Ghorbel E (2008) A viscoplastic constitutive model for polymeric materials. Int J Plast 24:2032–2058
20. Jin T, Zhou ZW, Shu XF, Wang ZH, Wu GY, Zhao LG (2016) Experimental investigation on the yield loci of PA66. Polym Test 51:148–150
21. Vural M, Rittel D, Ravichandran G (2003) Large strain mechanical behavior of 1018 cold-rolled steel over a wide range of strain rates. Metall Mater Trans A 34A:2873–2885